JOURNAL OF PROPULSION AND POWER
Vol. 35, No. 2, March–April 2019

Reduced Order Modeling of a Supersonic Flow Field

Kyle J. Woolwine* and Kenneth E. Jansen†
University of Colorado, Boulder, Colorado 80309
and
George Kopasakis‡ and Joseph W. Connolly§
NASA Glenn Research Center, Cleveland, Ohio 44135

DOI: 10.2514/1.B37064

This paper covers the development of a new reduced order model for supersonic flow fields. The name of the method is the small disturbance streamline method. Its purpose is to model the unsteady flow dynamics of 2-D or 3-D inviscid, supersonic flow fields in response to small-amplitude perturbations in a quasi-1-D model. The primary motivation of this research is focused on reduced order modeling of supersonic inlets to be used as part of a larger propulsion system or aero-propulso-servo-elastic model. Previous reduced order models have focused mainly on the internal duct portion of the inlets while using simple methods for the unsteady dynamics of the external compression portion. While this method is applicable to internal ducts without normal shocks, the main contribution is in modeling the external supersonic compression portion. Four test cases of increasing complexity are provided and compared with a chosen state-of-the-art method. All results are verified with a high-fidelity computational fluid dynamics code.

Nomenclature

A	=	cross-sectional area, m^2
c	=	speed of sound, m/s
c_p	=	specific heat at constant pressure, $kJ/(kg \cdot K)$
c_v	=	specific heat at constant volume, $kJ/(kg \cdot K)$
E_{tot}	=	total energy, kJ/kg
f	=	frequency of perturbation, Hz
H_{tot}	=	total enthalpy, kJ/kg
L^2	=	integrated relative L2 error
M	=	Mach number
$\hat{n}$	=	surface normal direction
p	=	static pressure, Pa
Q_i	=	flux variables
T	=	static temperature, K
t	=	time, s
U_i	=	conserved flow variables
u	=	speed, m/s
u_i	=	velocity component, m/s
x	=	length, m
$\boldsymbol{x}$	=	Cartesian vector
$\boldsymbol{x}$	=	truth solution
$\hat{\boldsymbol{x}}$	=	solution in question
γ	=	ratio of specific heats
δ	=	disturbance wave
δ_p	=	change in static pressure, Pa
δ_u	=	change in speed, m/s
δ_ρ	=	change in static density, kg/m^3
Θ	=	location angle, rad
μ	=	Mach angle
ρ	=	static density, kg/m^3
τ	=	time delay, s
Ω	=	domain

Superscripts

e	=	entropy wave
$+$	=	fast acoustic wave
$-$	=	slow acoustic wave
∞	=	freestream

Subscripts

i, j, k	=	Einstein notation
t	=	time derivative
tot	=	total property
x	=	spatial derivative

I. Introduction

SUPERSONIC inlets have a moderate degree of variation in their shape and flow field characteristics but they all are designed to perform the same basic function, which is to provide the compressor face of the turbo machinery with the required amount of subsonic flow in the most efficient way possible and with the least amount of distortion. Therefore, careful thought and design are dedicated to compressing the incoming air as close to isentropic as possible and with as little boundary-layer separation as possible. Depending on the flight regime and position of the engines, the shape of the inlet will vary to accomplish these objectives. However, in every case, the flow field at the design point is characterized by having oblique or conical shocks in the supersonic, external compression portion of the flow field, a normal shock that separates the supersonic and subsonic regimes, and a fast dynamic response to perturbations due to the high propagation speeds of disturbance waves. An example of an axisymmetric external compression inlet and its flow field features can be seen in Fig. 1.

In recent years, reduced order modeling of supersonic inlets has become an active area of research. In some cases, these models are created as a part of a larger propulsion system model [1] or as part of an aero-servo-elastic model (ASE) [2]. In these cases the goal is to study the coupled dynamics and create control laws for the integrated dynamic system. In other cases, the inlet model is created to develop controls algorithms to study the effect of perturbations on normal shock movement [3–5]. This is especially true for mixed compression inlets where inlet unstart or the expulsion of the normal shock is to be avoided. In either case, the reduced order inlet model must accurately capture the dynamic response of the system to either freestream or propulsion system perturbations in order to be a useful representation of the flow field. For this to happen, the model must accurately

Received 19 January 2018; revision received 22 July 2018; accepted for publication 5 September 2018; published online 12 December 2018.

*Ph.D. Student, Aerospace Engineering Department. Student Member AIAA.
†Professor, Aerospace Engineering Department. Associate Fellow AIAA.
‡Controls Engineer, Intelligent Control and Autonomy Branch. Member AIAA.
§Aerospace Engineer, Intelligent Control and Autonomy Branch. Senior Member AIAA.

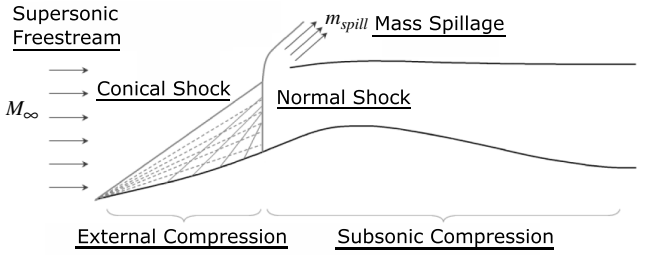

Fig. 1 Flow field features.

capture both the amplitude and the frequency response associated with the perturbations as they move through the flow field.

In most supersonic inlets, the presence of moderate to strong oblique shocks in the external compression supersonic flow field and the presence of a normal shock in the mixed subsonic and supersonic flow of the internal portion of the inlet have often times resulted in separate modeling approaches for the two portions of the inlet. For the internal duct portion, it has been shown that quasi-one-dimensional computational fluid dynamics (1-D CFD) and other reduced order methods can accurately model this portion of the flow field [1,6,7]. However, in previous models, the unsteady response of the external compression portion of the flow field has either been ignored or oversimplified [1,3–5,7]. Although it is true that the steady-state solution can be obtained with classic methods such as the oblique shock relations for 2-D inlets or the method of characteristics for axisymmetric inlets, the dynamic response of this portion of the flow field to perturbations is yet to be represented accurately on a reduced order level without resorting to linearizing high-fidelity CFD results [8,9].

In previous attempts by Ahsun [3] and MacMartin [5], this portion of the flow field has been approximated as near isentropic, where the oblique or conical shock has been ignored and this portion of the flow field has been modeled as part of the internal duct. This approach is problematic for inlets with moderate-strength oblique shocks as it ignores the shock's effect on the propagation of perturbations as well as the jump in entropy that occurs. Other approaches have modeled freestream perturbations to single flow field variables using a single time delay affecting only the perturbed variable [1,7]. The issue here, as shown by MacMartin [5], is that perturbations to single or multiple flow field variables create three disturbance waves in the form of a slow and fast acoustic wave and an entropy wave that affects every flow field variable downstream. Finally, each of these approaches assumes that disturbance waves can be modeled as instantaneous steps that move through the flow field. As will be seen in the current paper, this approach ignores the cone of influence downstream of the disturbance location and the fact that disturbances move along characteristic lines. This point becomes critical when applying sinusoidal disturbances.

Reduced order modeling in general has proven to be an important means of modeling complex parametric systems of equations. In many cases this involves a formal derivation of reduced basis matrices to represent the full system of equations. Popular methods include rational interpolation methods [10–12], balanced truncation methods [13,14], and proper orthogonal matrix decomposition [9,15–17]. Other methods such as those by Kopasakis et al. [1], Pilkhwal et al. [18], and Léonard and Adam [19] are *ad hoc* and rely on the knowledge of the underlying physics to create the reduced order model. The model developed herein falls into the category of the latter examples. In this case the higher-order system consists of the unsteady, 3-D Euler equations, restricted to supersonic flows, and the reduced order model is a quasi-1-D representation of that flow field.

The focus of this paper will be on modeling the external compression portion of the flow field of a supersonic inlet upstream of the normal shock as seen in Fig. 1. However, the method developed is general enough that it could be applied to the reduced order modeling of other supersonic flow fields. For most practical inlet cases, this method will need to be combined with other methods such as those detailed by Kopasakis et al. [1] to correctly model relevant features of the flow field such as normal shock movement and cowl lip spillage. The purpose here is to provide an accurate reduced order model of a region of supersonic inlet modeling that has been largely oversimplified or ignored. The ultimate engineering usefulness of this method, when combined with other modeling techniques, is expected to be in developing dynamically accurate reduced order models for control law development similar to those found in Ref. [1].

The method will build mainly on ideas by both Kopasakis et al. [1] and MacMartin [5]. The approach will be to apply small-amplitude, freestream perturbations to the primitive flow variables as planar disturbances, normal to the flow direction. These disturbances will then be converted to three freestream disturbance waves (slow acoustic, fast acoustic, and an entropy wave) using the method developed by MacMartin [5]. Steady-state solutions associated with each disturbance wave are then found using the method that is most efficient for the selected geometry. In some cases these steady-state solutions are obtained using high-fidelity CFD solutions and in others using simpler methods such as the method of characteristics. In all cases, the steady-state solutions are found by solving the Euler equations, as viscous effects are ignored. The time propagation of each disturbance wave is then found by averaging the local propagation speeds along streamlines in the flow field. The results of the method are verified in each case using a high-fidelity CFD code.

II. High-Fidelity CFD Verification

The parallel, hierarchic (second- to fifth-order accurate), adaptive, stabilized (finite-element) transient analysis (PHASTA) code has been chosen as the verification tool for the new reduced order model. PHASTA can be used to find the solution of compressible or incompressible flows. PHASTA (as well as its predecessor ENSA) was the first massively parallel unstructured grid, large eddy simulation (LES)/direct numerical simulation (DNS) code [20] and has been applied to flows ranging from verification benchmarks to cases of practical interest.

In PHASTA, flow computations are performed using a stabilized, semidiscrete finite element method for the transient, compressible, or incompressible Navier–Stokes partial differential equation (PDE) governing fluid flows. In particular, PHASTA employs the streamline upwind/Petrov-Galerkin (SUPG) stabilization method introduced in [21] to discretize the governing equations. The stabilized finite element formulation currently used has been shown to be robust, accurate, and stable on a variety of flow problems (see, e.g., [22,23]). In the flow solver (PHASTA), the Navier-Stokes equations (conservation of mass, momentum, and energy) plus any auxiliary equations (as needed for turbulence models or level sets in two-phase flow) are discretized in space and time. The discretization in space based on a stabilized finite element method leads to a weak form of the governing equations, where the solution (and weight function) are first interpolated using hierarchic, piecewise polynomials [23,24], and followed by the computation of integrals appearing in the weak form using Gauss quadrature. Implicit integration in time is then performed using a generalized-α method [25], which is second-order accurate and provides precise control of the temporal damping to reproduce Gear's method, Midpoint Rule, or any blend in between. On a given time step, the resulting nonlinear algebraic equations are linearized to yield a system of equations that are solved using iterative procedures. Although PHASTA is capable of solving the full Navier-Stokes equations, for the purposes of this paper, the 3-D Euler equations are being solved.

III. Assumptions and Background

The research contained in this paper covers the development of a new reduced order model for supersonic flow fields named the small disturbance streamline method (SDSM). Several assumptions are made in the development of the reduced order model. First, it is assumed that the entire flow field is supersonic. This assumption restricts the SDSM to the supersonic external compression portion of external compression and mixed compression inlets but may be applied to the entire inlet portion of a ramjet or scramjet, assuming

that there are no normal shocks present. Second, it is assumed that the flow field can be modeled as inviscid, which implies that no boundary-layer separation is expected to occur. For supersonic inlets this assumption is supported by the unsteady 3-D viscous CFD results from Chima et al. [26], which showed negligible boundary-layer separation in the flow of their simulations. Additionally, when boundary-layer separation occurs, it happens as a result of normal shock/boundary-layer interaction. This paper focuses on the region upstream of the normal, and so this is not a concern. Additionally, no communication is assumed to occur upstream through the boundary layer. As a result of this, it is assumed that the dynamics of the flow field are dominated by the inviscid flow. Next, it is assumed that all perturbations are applied as low-amplitude disturbances to one or more of the primitive flow variables. The amplitude is assumed to be small enough that the resultant disturbance waves can be modeled as acoustic and entropy waves. Finally, it is assumed that all perturbations are applied uniformly to the entire inflow plane. The purpose here is to mimic either atmospheric perturbations in a 1-D sense as shown by Kopasakis [27] or as a result of vehicle perturbations as shown by Ashun [3]. In either case, disturbances will be applied as small-amplitude perturbations to one or more of the freestream flow variables, either as step disturbance or sinusoidal disturbances. In general, supersonic inlets can experience a larger range of disturbances as a result of normal shock movement or compressor surge. Modeling that category of disturbance would require combining this method with other modeling techniques as mentioned previously.

Planar disturbances applied to the freestream can be thought of as a Riemann or shock tube problem. As shown by Knight [28] and observed by Opalski and Sajben [29], instantaneously applying a small perturbation to one or several flow field variables will cause the flow field to equilibrate through the propagation of three disturbance waves. A general Riemann problem will result in the creation of a shock wave, an expansion fan, and a contact surface wave if the difference in flow variables between the two initial states is high. However, for small amplitude differences, the resulting waves are a fast acoustic wave (δ^+), an entropy wave (δ^e), and a slow acoustic wave (δ^-). The states on either side of these disturbance waves can be found by solving the Riemann problem [28]. In a 1-D flow field, these waves will propagate with a time delay of τ^+, τ^e, and τ^-, respectively, as seen in Eq. (1) [5].

$$\tau^{\pm} = \int_{x_i}^{x_j} \frac{1}{c} \frac{1}{M \pm 1}\, \mathrm{d}x, \qquad \tau^{e} = \int_{x_i}^{x_j} \frac{1}{cM}\, \mathrm{d}x \tag{1}$$

where the speed of sound c is defined by

$$c = \sqrt{\gamma RT} \tag{2}$$

The upper limit of this assumption, that is, a disturbance large enough that it cannot be realistically modeled as resulting in two acoustic waves and an entropy wave, has not been explored. It is conjectured that this will occur when it instead produces a shock wave, an expansion fan, and a contact surface wave as in the case of the shock tube problem. For the purposes of this study, that is not considered an issue as the focus will be on small-amplitude disturbance resulting from atmospheric turbulence or small vehicle maneuvers.

An alternative method for representing this phenomenon is detailed by MacMartin [5]. In MacMartin's study, nondimensional perturbations to the flow variables (u, p, T, and/or ρ) are converted to equivalent fast acoustic (δ^+), entropy (δ^e), and slow acoustic (δ^-) wave disturbances using the conversion matrix in Eq. (3). At any point, the flow properties in between the waves can be found by converting a single disturbance wave to equivalent flow field perturbations using the conversion matrix in Eq. (4). Representing flow variable perturbations this way was found to be the most convenient method and is how disturbances will be represented throughout the rest of the paper.

$$\begin{bmatrix} 2\delta^+ \\ 2\delta^- \\ \delta^e \end{bmatrix} = \begin{bmatrix} 1 & \gamma M & 0 \\ 1 & -\gamma M & 0 \\ -1/\gamma & 0 & 1 \end{bmatrix} \begin{bmatrix} \frac{\delta p}{p} \\ \frac{\delta u}{u} \\ \frac{\delta \rho}{\rho} \end{bmatrix} \tag{3}$$

$$\begin{bmatrix} \left(\frac{\delta p}{p}\right) \\ \gamma M\left(\frac{\delta u}{u}\right) \\ \gamma\left(\frac{\delta \rho}{\rho}\right) \end{bmatrix} = \begin{bmatrix} 1 & 1 & 0 \\ 1 & -1 & 0 \\ 1 & 1 & \gamma \end{bmatrix} \begin{bmatrix} \delta^+ \\ \delta^- \\ \delta^e \end{bmatrix} \tag{4}$$

This view is accurate if the flow can be described in a 1-D sense but requires greater discussion for 2-D and 3-D flow fields. In general, point disturbances in 2-D or 3-D supersonic flow propagate along their cone of influence, defined by the local Mach angle μ, as defined by Eq. (5) [30].

$$\mu = \sin^{-1}\left(\frac{1}{M}\right) \tag{5}$$

This can be seen in Fig. 2, where a disturbance is emanating from point four and is propagating downstream at different values of time. From Fig. 3, it can be seen that at a given location C, within the cone of influence of a point upstream, defined by distance x and angle θ, the time that it takes the disturbance wave front to reach this point can be related to the local velocity u and speed of sound c. Using trigonometric identities, the following equation can be derived to relate these quantitates.

$$(c\Delta t)^2 = (u\Delta t)^2 + x^2 - 2(u\Delta t)x\cos(\theta) \tag{6}$$

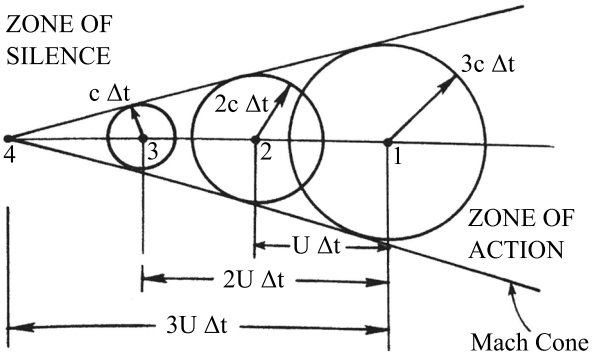

Fig. 2 Mach cone [31].

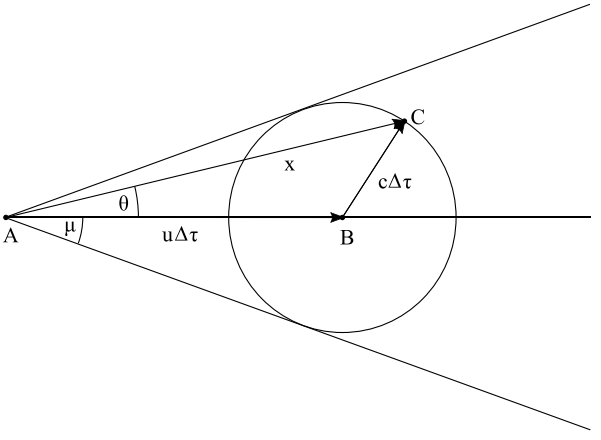

Fig. 3 Mach cone at a single point in time.

Equation (6) can then be rearranged to find the time delay at a given location within the cone of influence as seen in Eq. (7).

$$\Delta t = \frac{ux\cos(\theta)}{u^2 - c^2} - \sqrt{\left(\frac{ux\cos(\theta)}{u^2 - c^2}\right)^2 - \frac{x^2}{u^2 - c^2}} \tag{7}$$

From both Eq. (7) and Fig. 3 it is clear that the disturbance will reach points along the streamline($\theta = 0$) quicker than other points within the cone of influence. If it is imagined that a planar disturbance is replaced with a series of point disturbances, each with their own cone of influence, a more accurate picture of how disturbance waves move through 2-D and 3-D flow fields is formed. The perturbation will still move through the flow field as a series of disturbance waves; however, this view helps visualize how the waves distort as they move through the flow field at speeds relative to the local flow conditions. As a result, a given point within an external compression flow field will not see three distinct "step" waves predicted by the 1-D equations. Instead the response at a point will be due to the combined effect of every point up stream that has the downstream point within its cone of influence.

IV. Equivalent 1-D Flow Field

The purpose of this paper is to accurately and efficiently model how small-amplitude disturbances move through a 2-D or 3-D external compression flow field in the development of a quasi-1-D model. The strategy used will involve finding an equivalent 1-D representation of a 2-D or 3-D solution obtained from either CFD or another appropriate method. The 1-D representation will be developed at any given plane in the flow field normal to the incoming flow as seen in Fig. 4. So far it has been argued that this representation cannot be obtained using a simple 1-D model and instead requires a higher-fidelity representation. The question is then how to represent the 2-D or 3-D results within a quasi-1-D model. Varner et al. provided a method for accomplishing this in the Large Perturbation Inlet (LAPIN) Report [7]. However, this resource was found to contain a few errors, and so it is derived in full in the Appendix.

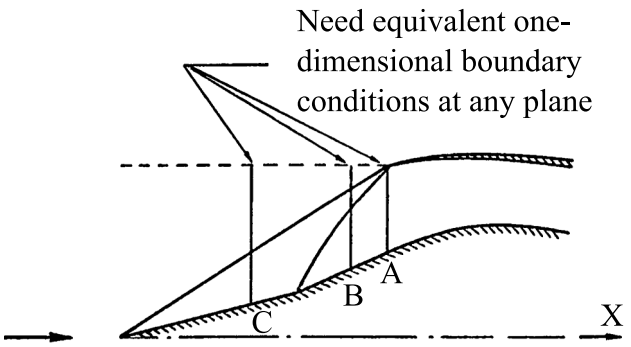

Fig. 4 Equivalent 1-D states [7].

V. Approach

The response of the supersonic flow field to small-amplitude disturbances can be described for an external compression inlet with the aid of Fig. 5. First the initial unperturbed steady-state solution is found ($U_i^{\infty}(\boldsymbol{x})$). Then the incoming flow variable disturbance, which is assumed to be planar and normal to the freestream flow direction, is decomposed into the three constituent disturbance waves (δ^+, δ^e, and δ^-) using Eq. (3). Note that, because the flow is supersonic and uniform upstream of this location, this marks the last location that the flow can realistically be modeled as a planar wave and be consistent with the model development herein. Each of these waves is then individually converted back into flow variable disturbances using Eq. (4). Next, each of these disturbances, represented in flow state variables, is used as freestream inputs to find a new temporary steady-state solution, resulting in four overall solutions for the entire flow field [Eq. (8)]. Note that any applicable method may be used to find the steady solution, such as a high-fidelity CFD solution or the method of characteristics. This process is illustrated with the example axisymmetric external compression flow field shown in Fig. 5.

$$\boldsymbol{U}_i(\boldsymbol{x}) = [U_i^{\infty}(\boldsymbol{x}), U_i^{+}(\boldsymbol{x}), U_i^{e}(\boldsymbol{x}), U_i^{-}(\boldsymbol{x})] \tag{8}$$

This process provides only the temporary steady-state solutions and not the full transient response. To solve for the transient response, the initial steady-state solution is interpolated along streamlines placed at constant inflow seed locations Δy, Δz as seen in the example geometry in Fig. 6a for a given z-axis location. The accuracy as a result of the chosen Δy and Δz spacing will be dependent on the numerical method chosen to evaluate the integral in Eq. (11). In general, the optimal spacing of Δy and Δz is problem dependent and can be determined analyzing the solution convergence. In Fig. 6a the bottom line represents the surface of a center body for an external compression inlet and the diagonal line represents the conical shockwave. Then the streamlines are looped through and Eq. (1) is

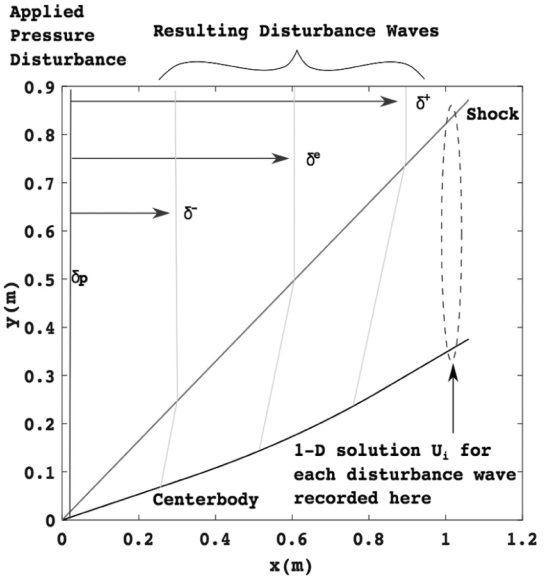

a) Disturbances in solution field

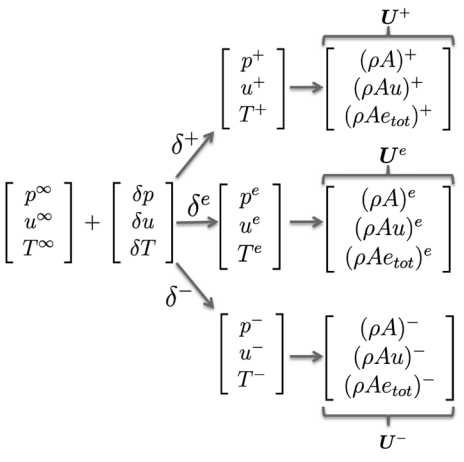

b) Flow variable decomposition

Fig. 5 Decomposition of disturbance into separate 1-D steady states.

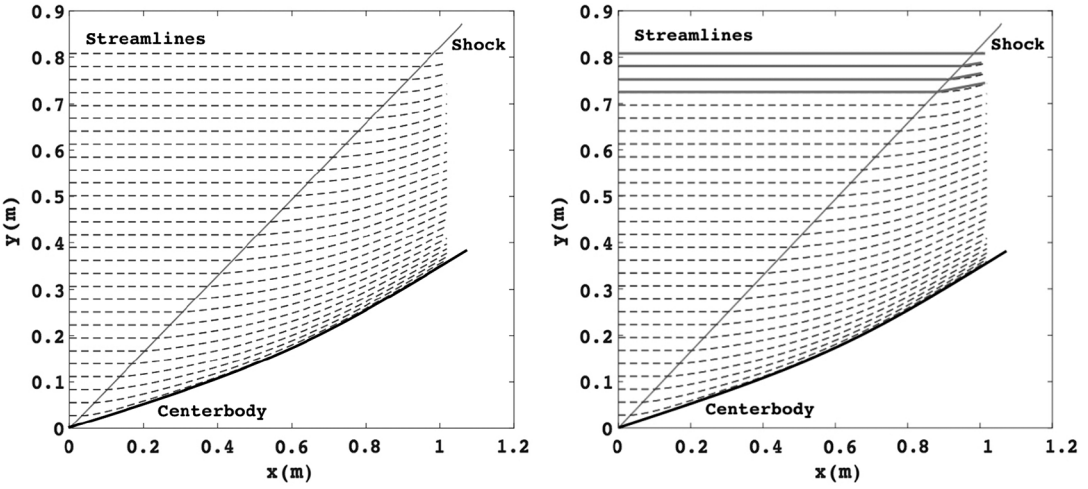

a) Streamlines at initial steady state **b) Example at time t_1**

Fig. 6 Streamlines in the solution field.

used to determine the time that it takes each disturbance wave to be translated along a given streamline. The "jth, kth" stream line is then assigned a vector seen in Eq. (9), which stores this information for each streamline that corresponds to the disturbance wave solutions in Eq. (8).

$$\boldsymbol{\tau}(j,k) = [t^{\infty}(\boldsymbol{x}), \tau^{+}, (\boldsymbol{x}), \tau^{e}(\boldsymbol{x}), \tau^{-}(\boldsymbol{x})] \tag{9}$$

Finally, the solution to an instantaneous flow variable step disturbance can be calculated by assuming that the 1-D representation of the flow field at a given x-location i transitions through each of the temporary steady-state solutions as the disturbance waves are propagated and distorted along the streamlines (Fig. 6a).

For example, consider the axisymmetric external compression flow field seen in Fig. 5a. Assume that at some time t_1 the fast acoustic wave has arrived at the location of interest labeled in this figure along some streamlines, but not others. This is seen in Fig. 6b, where the solid streamlines represent streamlines along which the fast acoustic wave has arrived at the exit plane and the dashed streamlines represent streamlines where it has not. At this time (t_1) the 1-D solution as a function of radial direction r can be represented as:

$$\boldsymbol{U}(t_1, r) = [\boldsymbol{U}^{\infty}(r_0), \boldsymbol{U}^{\infty}(r_1), \ldots, \boldsymbol{U}^{+}(r_{Nr-1}), \boldsymbol{U}^{+}(r_{Nr})] \tag{10}$$

Here, the terms with the "plus" superscript correspond to the steady-state solution of the fast acoustic wave and the terms with "∞" correspond to the initial unperturbed steady-state solution. The current equivalent 1-D solution at the measured exit plane can be calculated from Eq. (11). This process is repeated at every time step, allowing the solution to capture the transient response of the external compression flow field.

$$\boldsymbol{U}(t_1) = \frac{1}{A}\int_A \boldsymbol{U}(t_1, r)\,\mathrm{d}A \tag{11}$$

A similar process is used for sinusoidal freestream perturbations. In this case, however, the response is the result of the superposition of three overlapping sine waves phase shifted by their respective time delays. Again, the freestream flow variable perturbation is converted into the three principal disturbance waves and then converted into four separate steady-state solutions. Here the time vector is set in the same way as before, and the number of time steps and streamlines are looped over. At each time step, Eq. (12) is used to find the response for each streamline. Here τ is the time delay associated with each wave and the amplitude results from the difference between the steady state of each wave. Each term is added after the current time step exceeds the time delay for a given disturbance. As with the step disturbance, the final result is obtained by taking the area integral average of all of the streamlines at the exit plane using Eq. (11). This method will be referred to as the small disturbance streamline method (SDSM).

$$\begin{aligned}\boldsymbol{U}(t,r) = {} & \boldsymbol{U}^{\infty}(t,r) + (\boldsymbol{U}^{+}(t,r) - \boldsymbol{U}^{\infty}(t,r))\sin[2\pi f(t-\tau^{+})] \\ & + (\boldsymbol{U}^{e}(t,r) - \boldsymbol{U}^{+}(t,r))\sin[2\pi f(t-\tau^{e})] \\ & + (\boldsymbol{U}^{-}(t,r) - \boldsymbol{U}^{e}(t,r))\sin[2\pi f(t-\tau^{-})]\end{aligned} \tag{12}$$

VI. Results

The strength of the SDSM comes from the versatility of the numerical methods that it can be combined with. As mentioned, most of the computational work comes from obtaining the initial and temporary steady-state solutions associated with the resulting disturbance waves. However, the method used to obtain these solutions will be problem dependent. Four different test cases with increasing complexity have been chosen to illustrate this point. The chosen test cases are all 2-D in order to provide straightforward examples. However, there would be no added difficulty in applying the method to 3-D cases as long as the assumptions of the method are not violated. In every case, the results are compared to full unsteady CFD results using the PHASTA code for verification. For the last three test cases, MacMartin's model has been used for comparison. It was chosen as it is viewed as the best state-of-the-art model capable of this type of reduced order modeling. In the last case, some of the underlying assumptions of the MacMartin model are violated. It is included in this case to demonstrate the value of the SDSM. For each case the fluid being modeled is air and the values in Table 1 have been used.

The integrated relative L^2 error [Eq. (13)] is used to analyze the accuracy of SDSM method as compared with PHASTA.

$$L^2 = \frac{\int_{\Omega} \|\hat{\boldsymbol{x}} - \boldsymbol{x}\|_2\,\mathrm{d}\Omega}{\int_{\Omega} \boldsymbol{x}\,\mathrm{d}\Omega} \tag{13}$$

Here, $\hat{\boldsymbol{x}}$ is the solution in question and $\boldsymbol{x}$ is the "truth" solution or PHASTA solution in this case. The integrated relative L^2 error is a quantifiable method of difference throughout all of the examples. In

Table 1 Thermodynamic constants

Thermodynamic constant	Value used
c_p, kJ/(kg · K)	1.005
c_v, kJ/(kg · K)	0.718
R, J/(kg · K)	287
γ	1.4

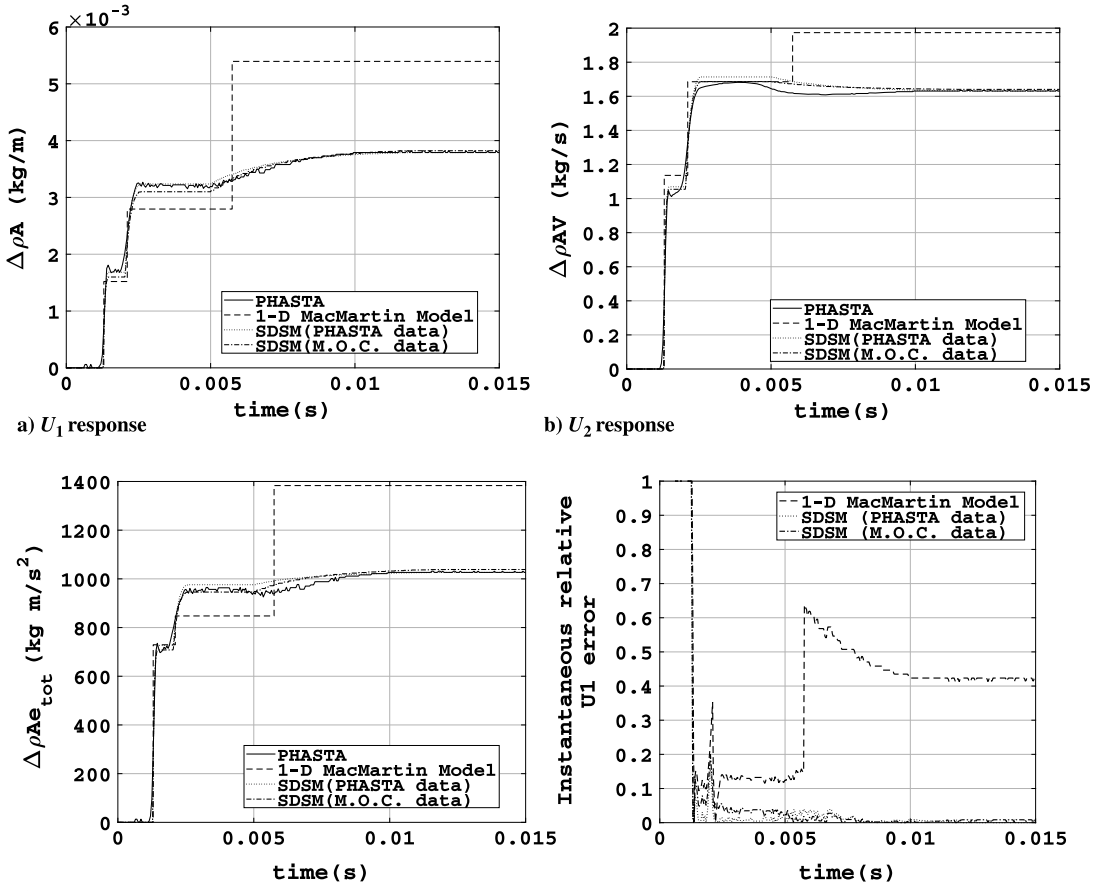

a) U_1 response b) U_2 response

c) U_3 response d) Instantaneous relative U_1 error

Fig. 7 Response to 100 Pa freestream pressure step.

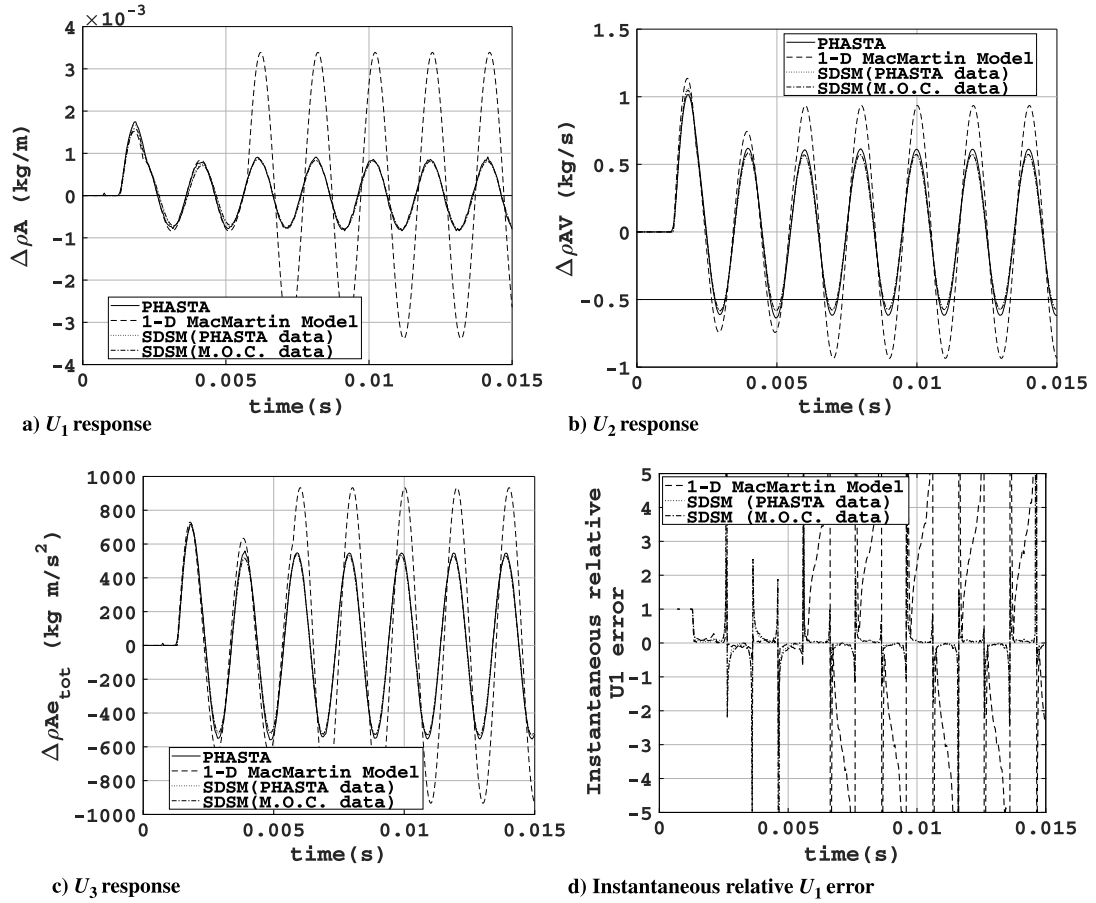

a) U_1 response b) U_2 response

c) U_3 response d) Instantaneous relative U_1 error

Fig. 8 Response to a 500 Hz, 100 Pa freestream pressure disturbance.

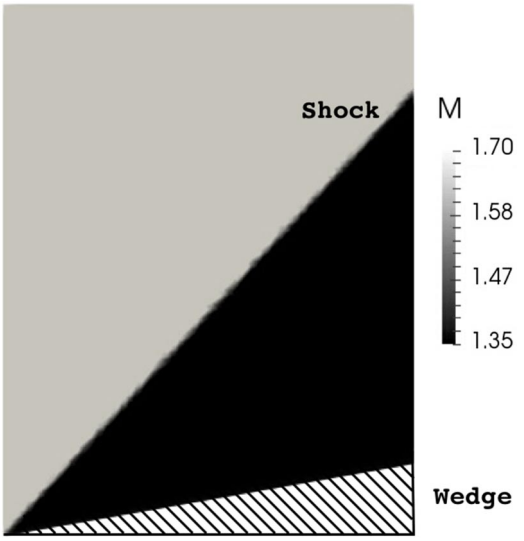

Fig. 9 Steady-state Mach number (PHASTA solution).

Table 2 Temporary inflow conditions for each disturbance wave due to pressure disturbance

Inflow variable	Unperturbed freestream	Fast acoustic wave (δ^+)	Entropy wave (δ^e)	Slow acoustic wave (δ^-)
M	1.7000	1.7020	1.7041	1.7000
p, Pa	11,597	11,647	11,647	11,697
T, K	216.65	216.92	216.38	216.65
u, m/s	501.57	502.48	502.48	501.57

Table 3 Two-dimensional wedge example relative L_2 error

Flow state variable	SDSM (oblique shock relations)	SDSM (PHASTA data)
U_1	0.0246	0.0199
U_2	0.0058	0.0046
U_3	0.0180	0.0119

the case of a sinusoidal disturbance, the amplitude and phase lag may be a more practical error measure but that is not possible for all of the cases. Furthermore, in the example where it is being compared with another method, MacMartin's, it provides a quantifiable means of comparing the two. Whether or not it is an acceptable absolute level of error will be application dependent. Lastly, a sample Matlab code that uses the SDSM and was used to obtain the SDSM(PHASTA data) results in Figs. 7 and 8 for the final two examples has been uploaded to GitHub at https://github.com/KyleWoolwine/ROM_SSFF_2018_Ex.

A. 2-D Wedge Flow

In the first case, supersonic freestream conditions are applied to a 2-D wedge with a deflection angle of 10 deg. This can be seen from the unperturbed steady-state solution in Fig. 9 (obtained using PHASTA). The freestream and boundary conditions used for this test can be seen in Table 2. To test the SDSM, a 100 Pa step in pressure is then applied to the steady-state solution at the inflow plane. When Eqs. (3) and (4) are used, this perturbation results in three new temporary sets of freestream inputs, in addition to the initial freestream conditions, as summarized in Table 2. Using the SDSM, the dynamic response at the exit plane ($x = 0.3$ m) is then calculated. For this example, both PHASTA and the theoretical oblique shock relations [30] were used to obtain the temporary steady states

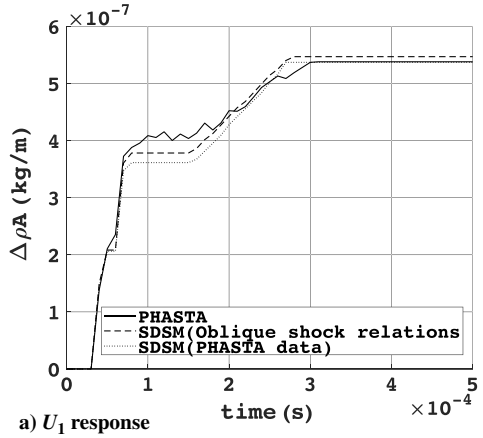

a) U_1 response

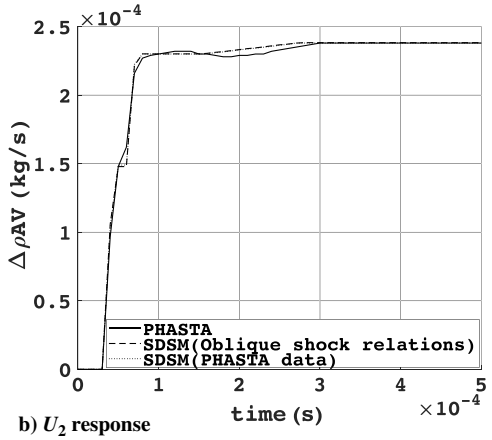

b) U_2 response

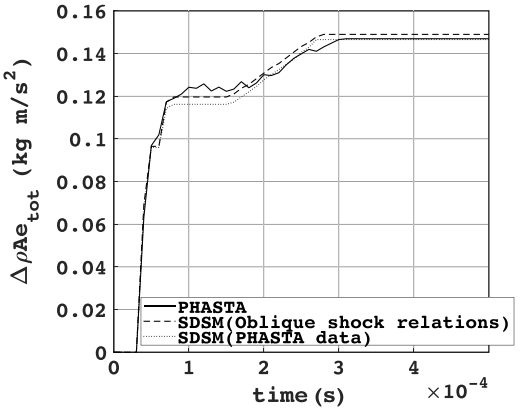

c) U_3 response

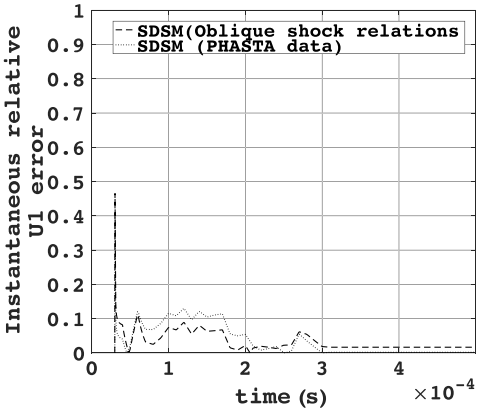

d) Instantaneous relative U_1 error

Fig. 10 Response to 100 Pa freestream pressure step.

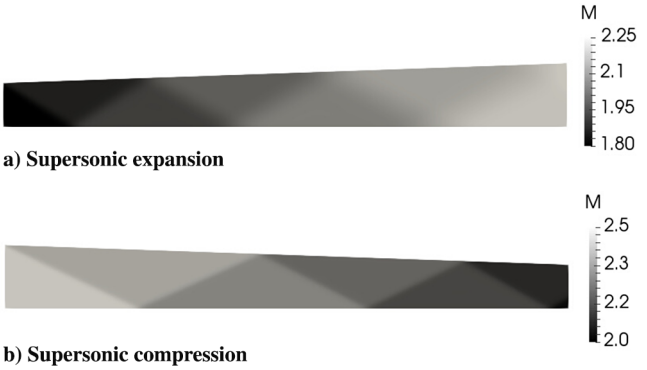

a) Supersonic expansion

b) Supersonic compression

Fig. 11 Two-dimensional duct test case PHASTA simulations.

Table 4 Two-dimensional test case boundary conditions

Boundary condition	Supersonic expansion	Supersonic compression
Inflow M	1.8	2.5
Inflow p, Pa	11,597	11,597
Inflow T, K	216.65	216.65
Slip walls	$\boldsymbol{V}\cdot\boldsymbol{n}=0, \partial T/\partial x_n = 0$	$\boldsymbol{V}\cdot\boldsymbol{n}=0, \partial T/\partial x_n = 0$

associated with each inflow condition. This is done in order to show the robustness of the method.

To verify the accuracy of this method, the 2-D wedge model in PHASTA (Fig. 9) is run to steady state using the first column of Table 2 and is then perturbed with the same 100 Pa step in freestream pressure. The equivalent 1-D representation is then recorded at a sampling frequency of 20,000 Hz using Eqs. (A6–A14).

Figures 10a–10c compare the response in conserved flow variables (U_i) at the exit plane, between the PHASTA simulations and the SDSM model. As can be seen from these figures the SDSM (using both PHASTA and the oblique shock relations) matched the results from the full unsteady PHASTA simulations with very little error. Not only is the amplitude of each wave predicted well but so is the transient response in between the arrival of each disturbance wave as can be seen in the relative instantaneous relative U_1 error in Fig. 10d. The instantaneous errors for U_2 and U_3 are not shown for clarity of presentation but their response is qualitatively similar to that of U_1. The low relative L^2 error seen in Table 3 confirms this observation. These results show that the SDSM provides nearly the same result as the high-fidelity CFD solution for this type of simulation.

B. Internal Duct

In the second test case, supersonic inflow conditions were applied to a 2-D internal duct with an area ratio of 1.454 between the inflow and outflow planes. The duct could be run as either supersonic expansion (Fig. 11a) or supersonic compression (Fig. 11b) depending on the choice of the inflow plane. For both of these simulations, PHASTA is run to steady state using the conditions in Table 4, where the flow remained supersonic throughout and no exit boundary conditions were needed. In both cases, after steady state is achieved, a step in pressure of 100 Pa is applied to the inflow plane and the response is measured at a distance of 1.05 m downstream. As with the previous case, the equivalent 1-D representation is recorded at a sampling frequency of 20,000 Hz using Eqs. (A6–A14).

From here, the results from PHASTA were compared with both the SDSM and the reduced order model detailed by MacMartin [5]. The model created by MacMartin (which will be referred to as the "1-D MacMartin model") is chosen because it is the most applicable

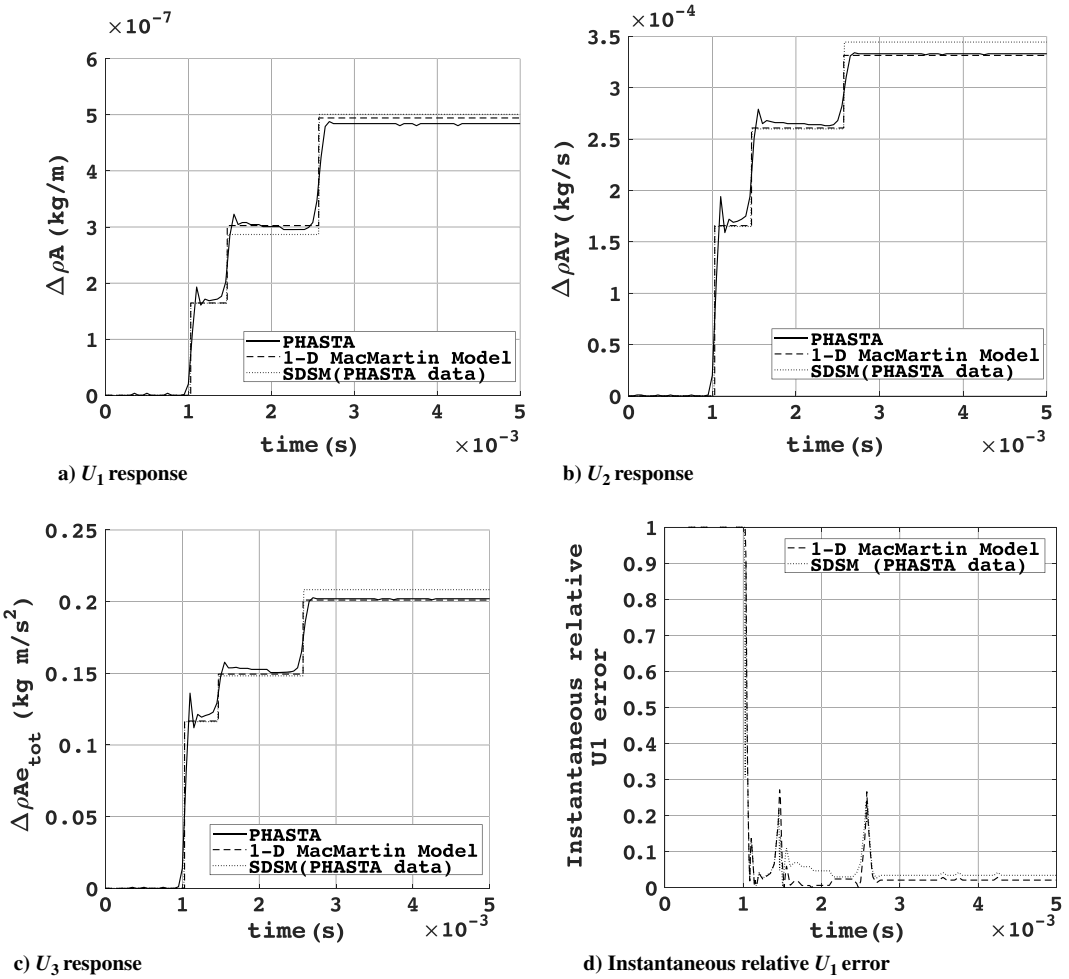

a) U_1 response

b) U_2 response

c) U_3 response

d) Instantaneous relative U_1 error

Fig. 12 Supersonic compression response to 100 Pa freestream pressure step.

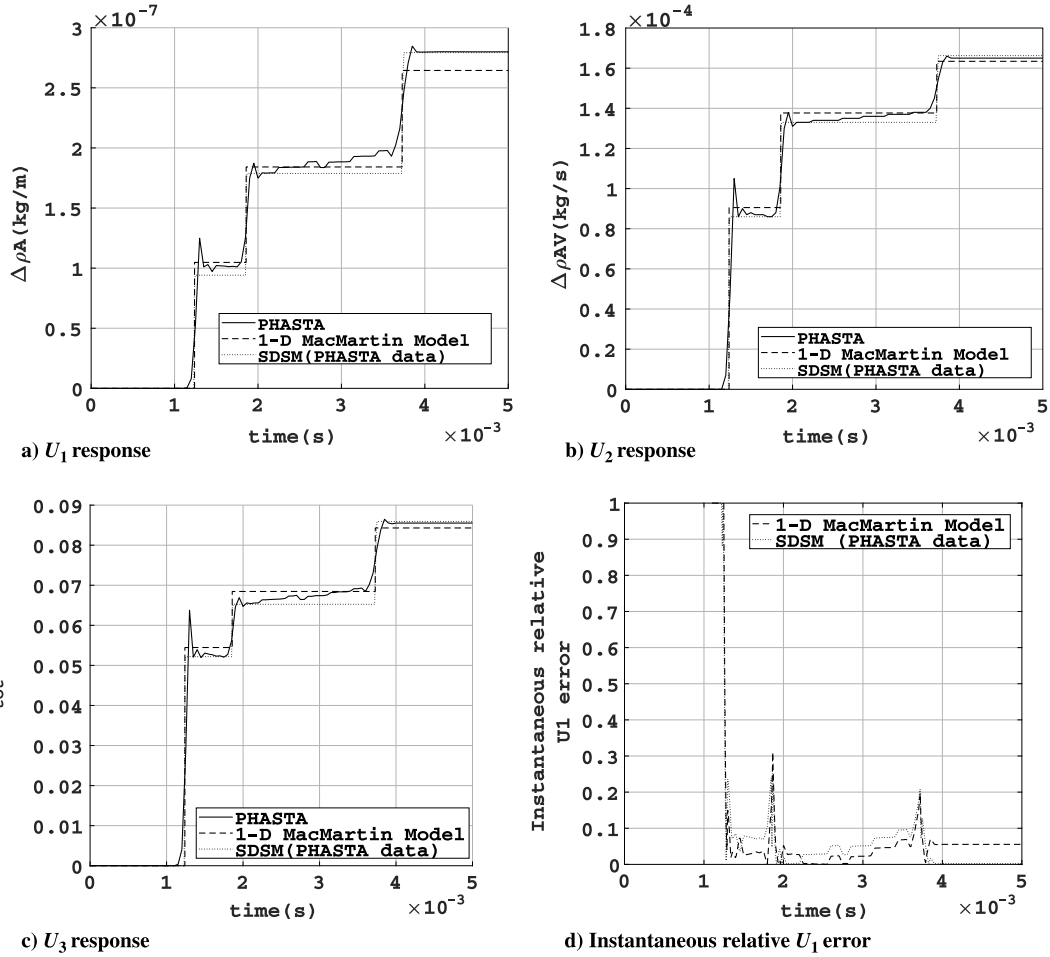

a) U_1 response b) U_2 response

c) U_3 response d) Instantaneous relative U_1 error

Fig. 13 Supersonic expansion response to 100 Pa freestream pressure step.

state-of-the-art reduced order inlet model that could be found. The MacMartin model is acceptable for these cases because it was developed specifically for internal duct quasi-1-D flows. Additionally, because the oblique shocks that are present here are weak and the flow states do not vary greatly between streamlines at any point in the streamwise direction, none of the assumptions for the MacMartin model are violated.

For this case, PHASTA is used to find the four steady-state solutions needed for the SDSM. Figure 12 details the response in conserved flow variables U_i to the applied inflow disturbance for the supersonic compression case. The results for the supersonic expansion case can be seen in Fig. 13. As can be seen in these figures, both methods did an excellent job of predicting both the amplitude and time delay of the disturbance waves created by the perturbation. Again, the instantaneous relative U_1 error is provided in Figs. 12d and 13d as a representation of the instantaneous error response for each case. In both cases, the level of L_2 error is very similar. From this it would seem that the model does an equal job handling flow dominated by either expansion fans or compression waves. This observation is supported by the error results in Table 5.

Table 5 Two-dimensional duct example relative L^2 error

	Supersonic compression		Supersonic expansion	
Flow state variable	1-D MacMartin model	SDSM (PHASTA data)	1-D MacMartin model	SDSM (PHASTA data)
U_1	0.0293	0.0461	0.0507	0.0410
U_2	0.0172	0.0388	0.0257	0.0245
U_3	0.0179	0.0390	0.030	0.0287

C. External Compression Inlet

In the final example, the external portion of an external compression inlet is used (Fig. 14). For this example, two test cases were created using freestream step and sinusoidal disturbances, respectively. For both test cases, the steady-state solution is first found using the same inflow state as in Sec. VI.A seen in the second column of Table 2.

In the first test case a step input in pressure of 100 Pa is added to the steady-state solution. Using the SDSM, this perturbation is used to find three new temporary steady-state solutions with the same freestream inputs seen in Table 2. For this example, both PHASTA and the method of characteristics (M.O.C.) [30] were used to obtain the temporary steady states. This is done in order to show the robustness of the method. With these solutions, the SDSM is used to find the dynamic response at the exit plane ($x = 1.089$ m) is calculated. The 1-D MacMartin model is also used, in order to compare the accuracy of SDSM to the closest state-of-the-art method.

To verify the accuracy of both methods, PHASTA is used to obtain the steady-state solution using the freestream conditions in Table 2 and is then perturbed with the same 100 Pa step in freestream pressure. The equivalent 1-D representation is then recorded at a sampling frequency of 20,000 Hz using Eqs. (A6–A14). Figures 7a–7c compare the response in conserved flow variables (U_i) at the exit plane, between the PHASTA simulations and the SDSM model. Again, the instantaneous relative U_1 error is provided in Fig. 7d as a representation of the instantaneous error response of the model. As can be seen from these figures the SDSM (using both PHASTA and the M.O.C.) matched the results from the full unsteady PHASTA simulations with very little error. Not only is the amplitude of each wave predicted well but so is the transient response in between the arrival of each disturbance wave, which is reflected in

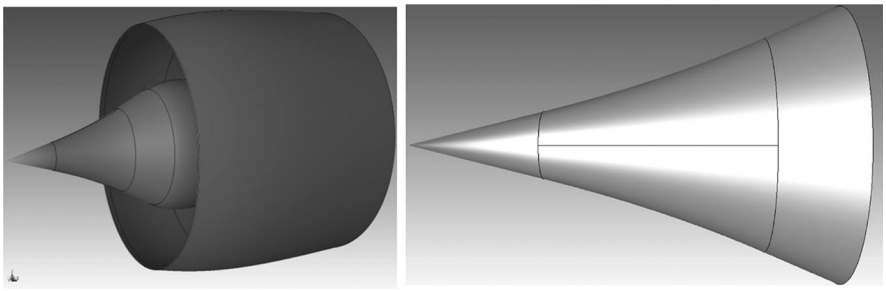

a) Entire inlet b) External compression portion

Fig. 14 Axisymmetric supersonic inlet model.

Fig. 7d. The 1-D MacMartin model, on the other hand, is not able to accurately capture this response.

This case illustrates some of the limits of the MacMartin method because two of its core assumptions are violated. First, the error in amplitude predicted for each disturbance wave can be attributed to the presence of the conical shockwave. The MacMartin model assumes that the flow is isentropic everywhere except across normal shocks. Here, the conical shock causes a steep increase in entropy generated, which causes the model to greatly overestimate the disturbance wave amplitude prediction. Second, the MacMartin model assumes that the disturbance waves, themselves, move as steps and are "nondispersive." This assumption is violated by the large gradient in flow variables orthogonal to the streamwise direction, which causes the disturbance waves to disperse as they propagate along streamlines at different local speeds. This is in contrast to the previous example in the internal duct where the disturbance waves moved as discrete step disturbances.

The SDSM, on the other hand, is able to aptly handle this example. By choosing an appropriate method such as the M.O.C. in this case to model the temporary steady states associated with each disturbance wave, no assumptions about the presence of conical or oblique shockwaves need to be made. Likewise, by tracking how each disturbance wave is carried along individual streamlines, the effect of the wave dispersion is captured accurately in an equivalent 1-D sense. These conclusions are reflected in Fig. 7 and the error analysis seen in Table 6.

For sinusoidal disturbances, it is crucial that both the amplitude and the time delay of each disturbance wave are captured due the constructive and destructive interference caused by the intersection of the waves. This is seen in the second test, where the same steady-state solution is perturbed using a 100-Pa-amplitude, 500-Hz freestream pressure disturbance. In this case, the same temporary steady solutions are used as in the previous test, as seen in Table 2, to determine the relative amplitudes of each wave expressed in Eq. (12). As before, both the M.O.C. and PHASTA were used to obtain the temporary steady states. Using the SDSM, the response in conserved flow variables (U_i) is seen in Figs. 8a–8c. As with the previous case, the response is compared with the full unsteady PHASTA simulation for verification. From these figures, it can be seen that the SDSM model again matches the PHASTA results with very little error. Likewise, the MacMartin model again fails to capture the response of the perturbation. This is not surprising because the same assumptions are violated that were in the last case. These statements are reflected in the error analysis seen in Table 7.

As with the previous examples, the instantaneous relative U_1 error is provided in Fig. 8d as a representation of the instantaneous error response of the model. The instantaneous error spikes as the PHASTA model crosses zero. This spiking behavior is unavoidable unless the model response is exactly the same as the PHASTA model. The main takeaway from this figure is the amount of error incurred in-between the zero crossing points for each model.

Table 6 External compression inlet step disturbance example relative L_2 error

Flow state variable	1-D MacMartin model	SDSM (PHASTA data)	SDSM (M.O.C. data)
U_1	0.3680	0.0104	0.0157
U_2	0.1594	0.0181	0.0155
U_3	0.2866	0.0161	0.0160

Table 7 External compression inlet sinusoidal disturbance example relative L_2 error

Flow state variable	1-D MacMartin model	SDSM (PHASTA data)	SDSM (M.O.C. data)
U_1	1.9921	0.0770	0.0951
U_2	0.4215	0.0666	0.0660
U_3	0.6423	0.0379	0.0448

Table 8 Computational expense

Efficiency metric	1-D MacMartin model	SDSM	PHASTA
ts/(procs × sec)	9.085	1.243	0.015
ts/(procs × sec) (without steady-state calc.)	15,000	1.440	0.029

D. Computational Expense

The normalized computational cost for each method was compared in terms of *time steps/(number of processors* × *seconds)* or *ts/(procs* × *sec)*. Using the external inlet results from Sec. VI.C, as an example, Table 8 displays the relative computational cost of the SDSM as compared with the other two featured methods. Here, the results are displayed with and without the cost of the steady-state solution needed for the unsteady solution. This was done because the MacMartin method requires a "nominal solution" to perturb in order to obtain the unsteady solution and could therefore be evaluated independently of the steady-state method chosen. The higher-fidelity Fortran/C++ code PHASTA results, which were run using four processors, took the longest to run and provided the best results. At the other end, the MacMartin method programmed in Matlab and ran using one processor took the shortest time to run, but provided unreliable results for this example. These two methods therefore help to bound the accuracy, complexity, and efficiency of the SDSM. The SDSM was programmed in Matlab and run using one processor. Although taking approximately 7 times longer to run than the MacMartin method, the SDSM provided similar results as PHASTA in a fraction of the time (1/83).

VII. Conclusions

An accurate dynamic reduced order model for supersonic flow fields has been developed called the small disturbance streamline method (SDSM). The method works by applying freestream disturbances as planar disturbances normal to flow direction at the inflow plane. These disturbances are converted to three freestream disturbance waves (slow acoustic, fast acoustic, and an entropy wave) and used to find the steady-state solutions associated with each wave. The time propagation of each disturbance wave is found by using a

streamline average. Finally, the transient response is found by transitioning through the steady-state solutions using the streamline averaged propagation speeds.

The results show that the SDSM is capable of handling a range of internal and external supersonic flow fields. Additionally, the SDSM was shown to work with a variety of established methods to obtain the steady-state solutions provided that they are appropriate methods. The SDSM performed on par with the current state-of-the-art reduced order 1-D MacMartin model and exceeded it in the external compression case. It should be noted that the 1-D MacMartin model was developed under the assumption that the flow is isentropic and only contains normal shocks, which is the likely cause for it being less accurate for the external compression case. This fact highlights the hypothesized usefulness of the SDSM, by showing the need for such a method.

For these reasons the SDSM can be used to develop inlet models for shock position control in the presence of flow disturbances such as atmospheric turbulence. This method can also be used to develop more accurate propulsion system dynamic models or aeroelastic models. More work is needed, however, to develop a complete supersonic inlet model to tie together the supersonic and subsonic flow regimes with moving computational domains.

Appendix: Equivalent 1-D Representation

The quasi-1-D Euler equations, along with the equation of state, which can be used to model the internal duct portion of supersonic inlets, are listed as Eqs. (A1–A4), which were taken from [32].

Continuity:

$$\frac{\partial}{\partial t}(\rho A) + \frac{\partial}{\partial x}(\rho A u_x) = 0 \tag{A1}$$

Momentum:

$$\frac{\partial}{\partial t}(\rho A u_x) + \frac{\partial}{\partial x}(\rho A u_x^2) = -A\frac{\partial p}{\partial x} \tag{A2}$$

Energy:

$$\frac{\partial}{\partial t}(\rho A E_{\text{tot}}) + \frac{\partial}{\partial x}(\rho A u_x H_{\text{tot}}) = -p\frac{\partial A}{\partial t} \tag{A3}$$

where, $E_{\text{tot}} = c_v T + (u_x^2/2)$ and $H_{\text{tot}} = c_p T + (u_x^2/2)$.

Equation of state:

$$p = \rho R T \tag{A4}$$

The continuity, momentum, and energy equations can be expressed generally as equation (A5):

$$\boldsymbol{U}_{,t} + \boldsymbol{F}_{,x} = \boldsymbol{S} \tag{A5}$$

where $\boldsymbol{U}$ is the flow state, $\boldsymbol{F}$ is the flux term, and $\boldsymbol{S}$ is the source term for each equation.

The output of a higher-order solution for an external compression flow field must be therefore represented in a way as to provide the correct upstream boundary conditions for the an internal duct model. For any given plane in the external flow field (A, B, or C in Fig. 4), the area integral average flux through that plane can be calculated with Eqs. (A6–A8).

Continuity:

$$Q_1 = \int_A \rho u \, \mathrm{d}A \tag{A6}$$

Momentum:

$$Q_2 = \int_A (p + \rho u V) \mathrm{d}A \tag{A7}$$

Energy:

$$Q_3 = \int_A (\rho E_{\text{tot}} + p) u \, \mathrm{d}A \tag{A8}$$

Here, V is the total velocity and u is the velocity component in the x direction. The integrals in these equations can be evaluated using any numerical integration routine. In this paper, the integral equations are evaluated numerically using a combination of the trapezoidal rule and Richardson extrapolation [33].

In terms of the conserved flow state variables $\boldsymbol{U}$, the Q equations can be represented as follows:

Continuity:

$$Q_1 = U_2 \tag{A9}$$

Momentum:

$$Q_2 = \left[(\gamma - 1)U_3 + \left(\frac{3-\gamma}{2}\right)\left(\frac{U_2^2}{U_1}\right)\right] \tag{A10}$$

Energy:

$$Q_3 = \left[\gamma U_3 - \left(\frac{\gamma - 1}{2}\right)\left(\frac{U_2^2}{U_1}\right)\right]\left(\frac{U_2}{U_1}\right) \tag{A11}$$

From here, the quasi-1-D conserved flow state variables $\boldsymbol{U}$ can be solved for using Eqs. (A12–A14).

$$U_2 = Q_1 \tag{A12}$$

$$\frac{U_2}{U_1} = \frac{-b \pm \sqrt{b^2 - 4ac}}{2a} \tag{A13}$$

$$U_3 = \frac{Q_2}{\gamma - 1} - \frac{3-\gamma}{2(\gamma - 1)} Q_1 \frac{U_2}{U_1} \tag{A14}$$

where

$$a = -\frac{(\gamma + 1)}{2(\gamma - 1)} Q_1 \tag{A15}$$

$$b = \frac{\gamma}{\gamma - 1} Q_2 \tag{A16}$$

$$c = -Q_3 \tag{A17}$$

Acknowledgments

This work was funded under the NASA GSRP fellowship program award number NNX12AK69H S03. This work used the Janus supercomputer, which is supported by the National Science Foundation (award number CNS-0821794) and the University of Colorado Boulder. The Janus supercomputer is a joint effort of the University of Colorado Boulder, the University of Colorado Denver, and the National Center for Atmospheric Research. Janus is operated by the University of Colorado Boulder. The authors would also like to thank Matt Lawry of the University of Colorado for advice concerning the error analysis in this paper.

References

[1] Kopasakis, G., Connolly, J., Paxson, D., and Woolwine, K., "Quasi 1D Modeling of Mixed Compression Supersonic Inlets," *50th AIAA Aerospace Sciences Meeting Including the New Horizons Forum and Aerospace Exposition*, AIAA Paper 2012-0775, 2012, p. 15. doi:10.2514/6.2012-775

[2] Connolly, J., Kopasakis, G., Carlson, J. R., and Woolwine, K., "Nonlinear Dynamic Modeling of a Supersonic Commercial Transport Turbo-Machinery Propulsion System for Aero-Propulso-Servo-

Elasticity Research," *51st AIAA/SAE/ASEE Joint Propulsion Conference, AIAA Propulsion and Energy Forum*, AIAA Paper 2015-4031, 2015, p. 12.
doi:10.2514/6.2015-4031

[3] Ahsun, U., "Dynamic Characterization and Active Control of Unstarts in a Near Isentropic Supersonic Inlet," Masters Dissertation, Aeronautics and Astronautics Department, MIT, Cambridge, MA, 2004.

[4] Dalle, D., Fotia, M., and Driscoll, J., "Reduced Order Models of 2D Supersonic Flow with Applications to Scramjet Inlets," *Journal of Propulsion and Power*, Vol. 26, No. 3, 2010, pp. 545–555.
doi:10.2514/1.46521

[5] MacMartin, D., "Dynamics and Control of Shock Motion in a Near-Isentropic Inlet," *Journal of Aircraft*, Vol. 41, No. 4, 2004, pp. 846–853.
doi:10.2514/1.416

[6] Smart, M., "Flow Modeling of Pseudoshocks in Backpressure Ducts," *AIAA Journal*, Vol. 53, No. 12, 2015, pp. 3577–3588.
doi:10.2514/1.J054021

[7] Varner, M., Martindale, W, Phares, W., Kneile, K., and Adams, J. C., "Large Perturbation Flow Field Analysis and Simulation for Supersonic Inlets," NASA TM-174676, 1986.

[8] Chicatelli, A., and Hartley, T., "A Method for Generating Reduced-Order Linear Models of Multidimensional Supersonic Inlets," NASA TM-207405, 1998.

[9] Willcox, K., Peraire, J., and White, J., "An Arnoldi Approach for Generation of Reduced-Order Models for Turbomachinery," *Computers & Fluids*, Vol. 31, No. 3, 2002, pp. 369–389.
doi:10.1016/S0045-7930(01)00046-9

[10] Baur, U., Beattie, C., Benner, P., and Gugercin, S., "Interpolatory Projection Methods for Parameterized Model Reduction," *SIAM Journal of Scientific Computing*, Vol. 33, No. 5, 2011, pp. 2489–2518.
doi:10.1137/090776925

[11] Gugercin, S., Antoulas, C., and Beattie, C., "H_2 Model Reduction for Large-Scale Linear Dynamical Systems," *SIAM Journal on Matrix Analysis and Applications*, Vol. 30, No. 2, 2008, pp. 609–638.
doi:10.1137/060666123

[12] Daniel, L., Siong, O. C., Chay, L. S., Lee, K. H., and White, J., "A Multiparameter Moment-Matching Model-Reduction Approach for Generating Geometrically Parameterized Interconnect Performance Models," *IEEE Transactions on Computer-Aided Design of Integrated Circuits and Systems*, Vol. 23, No. 5, 2004, pp. 678–693.
doi:10.1109/TCAD.2004.826583

[13] Benner, P., and Damm, T., "Lyapunov Equations, Energy Functionals, and Model Order Reduction of Bilinear and Stochastic Systems," *SIAM Journal on Control and Optimization*, Vol. 49, No. 2, 2011, pp. 686–711.
doi: 10.1137/09075041X

[14] Gugercin, S., and Antoulas, C., "A Survey of Model Reduction by Balanced Truncation and Some New Results," *International Journal on Control*, Vol. 77, No. 8, 2004, pp. 748–766.
doi:10.1080/00207170410001713448

[15] Carlberh, K., Bou-Mosleh, C., and Farhat, C., "Efficient Non-Linear Model Reduction Via a Least-Squares Petrov-Galerkin Projection and Compressive Tensor Approximations," *Numerical Methods in Engineering*, Vol. 86, No. 2, 2011, pp. 155–181.
doi:10.1002/nme.v86.2

[16] Lieu, T., and Farhat, C., "Adaptation of Aeroelastic Reduced-Order Models and Application to an F-16 Configuration," *AIAA Journal*, Vol. 45, No. 6, 2007, pp. 1244–1257.
doi:10.2514/1.24512

[17] Lieu, T., Farhat, C., and Lesoinne, M., "Reduced-Order Fluid/Structure Modeling of a Complete Aircraft Configuration," *Computational Methods in Applied Mechanical Engineering*, Vol. 195, Nos. 41–43, 2006, pp. 5730–5742.
doi:10.1016/j.cma.2005.08.026

[18] Pilkhwal, D. S., Ambrosini, W., Forgone, N., Vijayan, P. K., Saha, D., and Ferreri, J. C., "Analysis of the Unstable Behaviour of a Single-Phase Natural Circulation Loop with One-Dimensional and Computational Fluid-Dynamic Models," *Annals of Nuclear Energy*, Vol. 34, No. 5, 2007, pp. 339–355.
doi:10.1016/j.anucene.2007.01.012

[19] Léonard, O., and Adam, O., "A Quasi-One-Dimensional CFD Model for Multistage Turbomachines," *Journal of Thermal Science*, Vol. 17, No. 1, 2008, pp. 7–20.
doi:10.1007/s11630-008-0007-z

[20] Jansen, K. E., "A Stabilized Finite Element Method for Computing Turbulence," *Computational Methods in Applied Mechanical Engineering*, Vol. 174, Nos. 3–4, 1999, pp. 299–317.
doi:10.1016/S0045-7825(98)00301-6

[21] Brooks, A. N., and Hughes, T. J. R., "Streamline Upwind / Petrov-Galerkin Formulations for Convection Dominated Flows With Particular Emphasis on the Incompressible Navier-Stokes Equations," *Computational Methods in Applied Mechanical Engineering*, Vol. 32, Nos. 1–3, 1982, pp. 199–259.
doi:10.1016/0045-7825(82)90071-8

[22] Taylor, C. A., Hughes, T. J. R., and Zarins, C. K., "Finite Element Modeling of Blood Flow in Arteries," *Computational Methods in Applied Mechanical Engineering*, Vol. 158, Nos. 1–2, 1998, pp. 155–196.
doi:10.1016/S0045-7825(98)80008-X

[23] Whiting, C. H., and Jansen, K. E., "A Stabilized Finite Element Method for the Incompressible Navier-Stokes Equations Using a Hierarchical Basis," *International Journal of Numerical Methods in Fluids*, Vol. 35, No. 1, 2001, pp. 93–116.
doi:10.1002/(ISSN)1097-0363

[24] Whiting, C. H., Jansen, K. E., and Dey, S., "Hierarchical Basis in Stabilized Finite Element Methods for Compressible Flows," *Computational Methods in Applied Mechanical Engineering*, Vol. 192, Nos. 47–48, 2003, pp. 5167–5185.
doi:10.1016/j.cma.2003.07.011

[25] Jansen, K. E., Whiting, C. H., and Hulbert, G. M., "A Generalized-α Method for Integrating the Filtered Navier-Stokes Equations with a Stabilized Finite Element Method," *Computational Methods in Applied Mechanical Engineering*, Vol. 190, Nos. 3–4, 2000, pp. 305–319.
doi:10.1016/S0045-7825(00)00203-6

[26] Chima, R., Conners, T., and Wayman, T., "Coupled Analysis of an Inlet and Fan for a Quiet Supersonic Jet," *48th AIAA Aerospace Sciences Meeting Including the New Horizons Forum and Aerospace Exposition*, AIAA Paper 2010-479, 2010, p. 13.
doi:10.2514/6.2010-479

[27] Kopasakis, G., "Modeling of Atmospheric Turbulence as Disturbances for Control Design and Evaluation of High Speed Propulsion Systems," *Journal of Dynamic Systems, Measurement, and Control*, Vol. 134, No. 2, 2011, p. 12.
doi:10.1115/1.4005368

[28] Knight, D., *Elements of Numerical Methods for Compressible Flows*, 1st ed., Cambridge Univ. Press, Cambridge, MA, 2006, pp. 19, 136.

[29] Opalski, A., and Sajben, M., "Inlet/Compressor System Response to Short-Duration Acoustic Disturbances," *Journal of Propulsion and Power*, Vol. 18, No. 4, 2002, pp. 922–932.
doi:10.2514/2.6018

[30] Anderson, J., *Modern Compressible Flow: with Historical Perspective*, 3rd ed., McGraw–Hill Education (India), New Delhi, India, 2013, pp. 230–300.

[31] Kundu, P. K., and Cohen, I. M., *Fluid Mechanics*, 4th ed., Elsevier Academic Press, Burlington, MA, 2008, pp. 750–752.

[32] Anderson, J., *Computational Fluid Dynamics: The Basics with Applications*, 1st ed., McGraw–Hill Series, Singapore, 1995, pp. 157–180.

[33] Richarson, L. F., "The Approximate Arithmetical Solution by Finite Differences of Physical Problems Involving Differential Equations, with an Application to the Stresses in a Masonry Dam," *Philosophical Transactions of the Royal Society A: Mathematical, Physical and Engineering Sciences*, Vol. 210, Nos. 459–470, 1911, pp. 307–357.
doi:10.1098/rsta.1911.0009

V. Raman
Associate Editor